Assessing the Provision of Ancillary Services Considering BES Capacity Degradation

Kalliopi D. Pippi
Dept. of Electr. & Comput. Eng.
Democritus University of Thrace
Xanthi, Greece
kpippi@ee.duth.gr

Georgios C. Kryonidis
Dept. of Electr. & Comput. Eng.
Aristotle University of Thessaloniki
Thessaloniki, Greece
kryonidi@ece.auth.gr

Angelos I. Nousdilis
Dept. of Electr. & Comput. Eng.
Aristotle University of Thessaloniki
Thessaloniki, Greece
angelos@ece.auth.gr

Theofilos A. Papadopoulos
Dept. of Electr. & Comput. Eng.
Democritus University of Thrace
Xanthi, Greece
thpapad@ee.duth.gr

***Abstract*—The ever-increasing penetration of distributed renewable energy sources, e.g., photovoltaics (PVs), poses new technical challenges, jeopardizing the reliable operation of power systems. For this reason, battery energy storage (BES) are situated alongside PV systems, to provide ancillary services (ASs) to system operators. However, BES operation is often limited due to the restricted number of operating cycles. In this paper, a methodology for the assessment of the provision of voltage regulation and power smoothing services by PV-BES systems is presented, taking into account the capacity degradation of BES. The proposed framework involves quasi-static simulations incorporating the operating conditions of the distribution network. A battery aging model is used to estimate the BES capacity loss caused by both the calendar and the cyclic aging mechanisms. The updated BES capacity sets new constraints on its operation and consequently influences the efficiency of the provided ASs.**

***Index Terms*—Ancillary services, battery energy storage systems, capacity degradation, power smoothing, renewable energy sources, voltage regulation.**

I. Introduction

A. Motivation and Background

Currently, the conventional passive distribution networks (DNs) are gradually converted to active systems, due to the advent of distributed renewable energy sources (DRESs), especially photovoltaics (PVs) [1]. This transition from the passive to active operation of DNs contributes to the development of new ancillary services (ASs) that can exploit the functionalities of network assets, e.g., battery energy storage (BES) systems, DRES, etc., to tackle long-term power quality problems related to the steady operation of DNs [2]. Voltage regulation (VR) and active power smoothing (PS) are considered as the most important ASs within the DN premise [3].

The research work was supported by the Hellenic Foundation for Research and Innovation (H.F.R.I.) under the "First Call for H.F.R.I. Research Projects to support Faculty members and Researchers and the procurement of high-cost research equipment grant" (Project Number: HFRI-FM17-229).

K. D. Pippi and T. A. Papadopoulos are with the Power Systems Laboratory, Department of Electrical and Computer Engineering, Democritus University of Thrace, Xanthi 67100, Greece (e-mail: kpippi@ee.duth.gr; thpapad@ee.duth.gr).

G. C. Kryonidis and A. I. Nousdilis are with the School of Electrical and Computer Engineering, Aristotle University of Thessaloniki, Thessaloniki 54124, Greece (e-mail: kryonidi@ece.auth.gr; angelos@auth.gr).

B. Relevant Literature

Regarding VR, a wide range of VR methods has been proposed in the literature. In [4], the well-established $Q(V)$ and $P(V)$ droop-based decentralized control schemes are combined to adjust the active power of BES systems and the reactive power of DRES to control network voltages by prioritizing the use of active against reactive power. However, intense BES utilization for providing ASs has a negative effect on their lifetime expectancy. In addition, in [5] an optimization-based central control strategy is developed to determine the operating points of BES and DRES in order to constrain the voltage levels within predefined limits. However, the effect of the BES operation on the BES aging mechanism has not been investigated in none of [4] and [5]. This is taken into account in the optimization model of [6] to flexibly control the battery charging/discharging power of electric vehicles, considering the voltage regulation of the power grid via the use of the on-load tap changer and bank capacitors.

Respectively, various PS techniques have been also introduced to mitigate the output power fluctuations caused by the volatile and intermittent operation of DRESs. In [7], a ramp-rate limitation (RRL) method is employed by BES systems and in [8], a high-pass filter with adjustable cutoff frequency is utilized to smooth the output power of the DRES and achieve fair state-of-charge (SoC) sharing among the network BES units. However, both [7] and [8], do not take into account BES capacity degradation. In [9], the impact of the most well-established PS methods on the BES system long-term performance is investigated. By performing a systematic parametric analysis, it has been shown that the RRL methods outperform the filtering-based techniques in terms of BES sizing, smoothing, and capacity degradation.

Citation information, DOI: 10.1109/SEST53650.2022.9898493

Most of the above studies [4], [5], [7]–[9] solely focus on investigating one particular type of AS and most importantly neglecting BES capacity degradation. This is merely done in [10], where the provision of multiple ASs considering BES degradation has been examined, but from an economic evaluation perspective.

C. Contributions

Based on the above analysis, it can be deduced that literature lacks of an assessment framework where the impact of the BES degradation on the long-term performance of the provided ASs can be examined. To fill this gap, this paper investigates the provision of ASs by PV-BES systems within a multi-services perspective. A methodology to evaluate the provision of VR and PS services is proposed. The proposed methodology combines a calendar and cyclic battery degradation model with quasi-static simulations to replicate the practical operating conditions of the low-voltage (LV) DN. This is dictated to improve the accuracy of the final evaluation results. More explicitly, the cycle-counting algorithm of [11] is adopted to estimate the BES system capacity fading, setting in turn technical constraints to BES operation and consequently to the effectiveness of the provided ASs.

II. Methodology

To evaluate the provision of VR and PS ASs by PV-BES systems to DNs a quasi-static simulation model is developed. Long-term performance analysis, e.g., 20 years, is conducted on the basis of multiple 24-h time simulations. Special emphasis is given on the modelling endeavor of the BES system by embedding a battery degradation algorithm into the simulation model. An overview of the proposed methodology is depicted in the flowcharts of Figs. 1 and 2 and in brief involves the following main steps:

- **Step 1**: Import PV, load, BES data and network topology.
- **Step 2**: To alleviate PV output power fluctuations during cloudy days an RRL-based PS algorithm is employed.
- **Step 3**: A day-ahead planning algorithm is applied to estimate the available BES capacity and ensure the effective participation of PV-BES systems in VR actions of the next day.
- **Step 4**: Quasi-static simulations are conducted. To mitigate possible voltage violations, a modified version of the $Q(V) - P(V)$ droop-based algorithm [4], [12] is used.

Steps 1-4 are repeated for a number of days in sequence (See Fig. 2) to create a multi-day simulation pattern of time period T_{qss}.

- **Step 5**: The simulation pattern of T_{qss} is used to evaluate the BES capacity loss [11] (See Fig. 2). The BES aging analysis is conducted regularly with a time period, T_{BES}; T_{BES} can vary from a day to several years depending on the preferred analysis accuracy. The BES capacities are updated and imported in Step 1 to perform the quasi-static simulations required for the next T_{BES}, and the elapsed analysis period (T_{LtP}) is updated accordingly. Note that, if $T_{\text{qss}} < T_{\text{BES}}$, the multi-day pattern is reiterated up to T_{BES}.

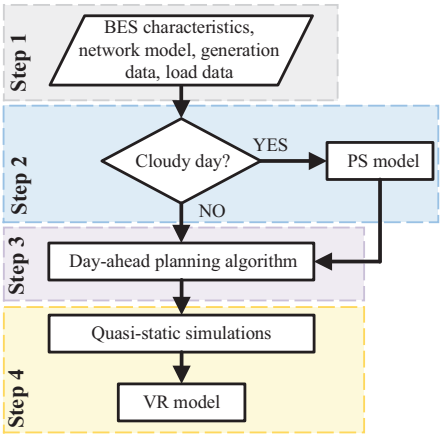

Fig. 1. Flowchart of the proposed methodology (quasi-static simulations).

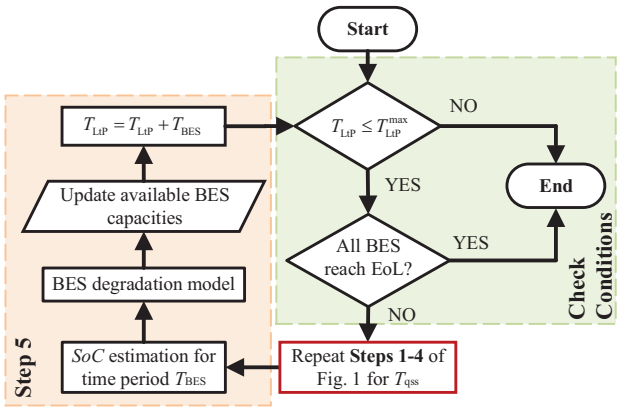

Fig. 2. Flowchart of the proposed methodology (BES aging analysis).

The above procedure is repeated for every T_{BES} till either the end of the long-term analysis period ($T_{\text{LtP}}^{\max}$) is reached or the capacity of all BES units is less than 80 % of their nominal value, indicating their end of life (EoL) [13] (See Fig. 2). In case a BES reaches the EoL earlier than the rest units, it is not considered in the simulation model for the rest of $T_{\text{LtP}}^{\max}$.

A. Voltage Regulation Method

The modified $Q(V) - P(V)$ droop control scheme of Fig. 3 is applied to the local controller of the PV-BES systems to regulate the positive-sequence network voltages as imposed by the recently revised IEEE 1547 Standard [14]. Specifically, this control scheme constitutes one of the most widely known VR methods and it can be readily integrated to commercial inverters. According to $Q(V) - P(V)$, the output reactive power (Q) of either the PV or the BES and the output active power (P) of the BES are adjusted according to the positive-sequence voltage (V) at the point of interconnection of each PV-BES system with the grid. Here, V_1, V_2, V_3, V_4, V_5, V_6 denote the voltage thresholds of each droop curve, $V_{\min}$ and $V_{\max}$ stand for the minimum and maximum permissible voltage limits, and $P_{\max}$ and $Q_{\max}$ are the maximum active and reactive power, respectively, that can be used by the BES system and/or the PV. Note that, $P_{\max}$ is determined by the

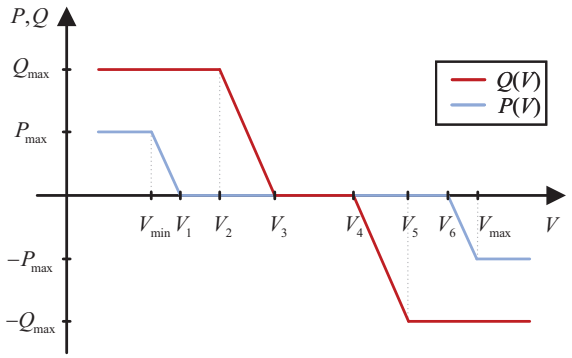

Fig. 3. $Q(V) - P(V)$ droop control curve. A positive P (or Q) value indicates injection to the grid.

rated power of the BES system, and $Q_{\max}$ is calculated by considering the reactive power capability as follows:

$$Q_{\max} = \sqrt{S^2 - P^2} \tag{1}$$

where S denotes the rated apparent power of either the PV or BES and P is the corresponding output active power.

The main difference between the modified and the original approach [12] lies on the use of the BES active power to control the output active power of the PV-BES system, avoiding the PV active power curtailment and the loss of green energy. Contrary to [4], priority is given to the use of the reactive power against active power to reduce BES utilization. This is attained by setting narrower voltage thresholds for the activation of the reactive power control ($Q(V)$) compared to the active power control ($P(V)$) as shown in Fig. 3.

The main triggering signal for the use of the BES system active power in the VR process is the positive-sequence voltage. As no other inputs are used, the method cannot ensure the availability of BESs to provide active power support since their storage capability is limited due to their sizing constraints. To overcome this issue, a day-ahead planning algorithm is adopted aiming to ensure that sufficient amount of energy can be provided or stored by the BESs during the next day and consequently their effective participation in the VR process. In particular, considering overvoltage mitigation, the proposed algorithm works as follows. Forecasted day-ahead generation and consumption profiles are used in order to perform quasi-static simulations employing the proposed VR method. By the conducted simulations, the required storage range (SR), i.e., the amount of energy that will be stored during the VR process by each BES in the next day, is predicted. To mitigate possible miscalculations caused by the forecast errors a safety factor (sf) is assumed to calculate the final value of SR. Subsequently, a discharging process with constant power is applied to each BES with non-zero SR during no-generation periods to reach the required storing capability. Note that a similar process can be followed for undervoltage mitigation.

B. Power Smoothing Technique

According to [9], RRL-based methods can assure effective PS with reduced BES utilization leading to increased BES lifetime. For this reason, in order to smooth out the PV output power fluctuations an enhanced RRL-based method is adopted [7]. The RRL control scheme limits the ramp rate of the PV output power, P^t_{mpp}, at each time instant, t, to prevent the violation of the maximum, $RR_{\max}$, and minimum, $RR_{\min}$ permissible ramp rates. Assuming that P^t_{input} is the power inserted to the RRL control, the ramp rate of the current time instant, RR^t, is given by (2):

$$RR^t = \frac{P^t_{input} - P^{t-\Delta t}_{sm}}{\Delta t} \tag{2}$$

where $P^{t-\Delta t}_{sm}$ is the smoothed value of the previous time instant. The RRL control calculates the smoothed PV power that will be injected into the grid, P^t_{sm}, as in (3):

$$P^t_{sm} = \begin{cases} P^{t-\Delta t}_{sm} + \Delta t \cdot RR_{\min}, & RR^t \leq RR_{\min} \\ P^{t-\Delta t}_{sm} + \Delta t \cdot RR^t, & RR_{\min} < RR^t < RR_{\max} \\ P^{t-\Delta t}_{sm} + \Delta t \cdot RR_{\max}, & RR^t \geq RR_{\max} \end{cases} \tag{3}$$

In this paper, the conventional RRL method is enhanced by introducing a feedback loop [7], as presented in Fig. 4, to recover the battery SoC towards a pre-specified level. This way the BES is always able to smooth out both positive and negative PV output variations. To achieve this, a feedback power, P^t_{fb}, defined in (4), is subtracted from P^t_{mpp} and the resulted power is used as input to the RRL control block.

$$P^t_{fb} = k(E^{ref}_{bat} - E^t_{bat}) \tag{4}$$

Here, E^t_{bat} is the energy stored in the battery at t, E^{ref}_{bat} is a reference value of E^t_{bat} used for SoC recovery, and k is the proportional gain set to 2.

The BES charges/discharges accordingly at a rate equal to P^t_{bat} to cover the difference between the actual and the targeted smoothed PV output. The integration of P^t_{bat} considering also the charging or discharging efficiency (η_{ch} or η_{dch}) provides the energy stored to/drained from the battery, that is utilized by the feedback control loop.

C. BES Degradation Model

The algorithm for the evaluation of the battery degradation within time period T_{BES} is illustrated in Fig. 5. The aging model for lithium-ion batteries of [11] is adopted to assess the capacity loss, considering both the calendar and the cyclic aging process of the battery cells. The calendar aging mechanism over period T_{BES} is modeled by the calendar degradation factor, f_{cal}, and is a function of the average SoC ($\overline{SoC}$) and the average battery temperature ($\overline{T}$) over T_{BES}. The cyclic degradation over the i-th charging-discharging cycle, f^i_{cyc}, depends on the depth of discharge (DoD), the $\overline{SoC}$, and the $\overline{T}$ of the cycle. The cyclic aging within T_{BES} is calculated as the sum of the capacity degradation caused by all cycles within T_{BES}. The DoD, the $\overline{SoC}$, the $\overline{T}$ of each cycle and the total number of irregular cycles are determined from SoC timeseries by using the rainflow algorithm [15]. Finally, the capacity degradation rate over T_{BES}, $L^{T_{\text{BES}}}$, is obtained by (5):

$$L^{T_{\text{BES}}} = 1 - \alpha_{sei} e^{-\beta_{sei} f_d} - (1 - \alpha_{sei}) e^{-f_d}. \tag{5}$$

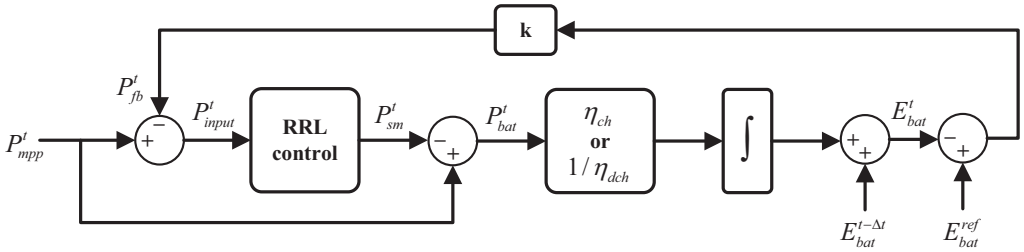

Fig. 4. Enhanced RRL-based PS technique with SoC recovery.

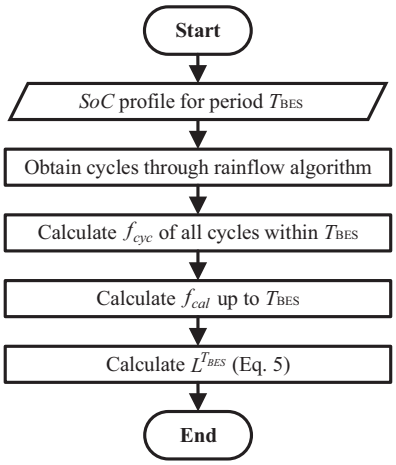

Fig. 5. Algorithm for the analysis of BES capacity degradation.

where α_{sei} and β_{sei} are parameters determined by experimental data and f_d is the overall degradation factor, calculated according to (6), for all cycles N within T_{BES}.

$$f_d = f_{cal} + \sum_{i}^{N} f^i_{cyc} \tag{6}$$

The analysis of the capacity fading is conducted at the end of each time period T_{BES} and the updated available capacity ($E^T_{\max}$) is derived by:

$$E^{T_{\text{BES}}}_{\max} = (1 - L^{T_{\text{BES}}}) E^0_{\max} \tag{7}$$

where $E^0_{\max}$ is the initial BES capacity.

III. Numerical Results

A. System Under Study

To evaluate the performance of the PS-VR methodology, quasi-static simulations are performed in OpenDSS [16] by using the IEEE European LV test feeder [17]. The original test feeder is modified by adding 32 PV-BES systems; the single-line diagram of the network is depicted in Fig. 6. The installed PV-BES systems are divided into two groups; BT1 consists of PV-BES units used only for PS and BT2 employs PV-BESs providing both PS and VR services. The connection node and the capacity of PVs and BES are summarized in Tables I and II, respectively; they have been determined for demonstration purposes of the method. Regarding the PV-BES operating characteristics, the power factor of PVs and BESs is considered equal to 0.85, the minimum ($SoC_{\min}$) and

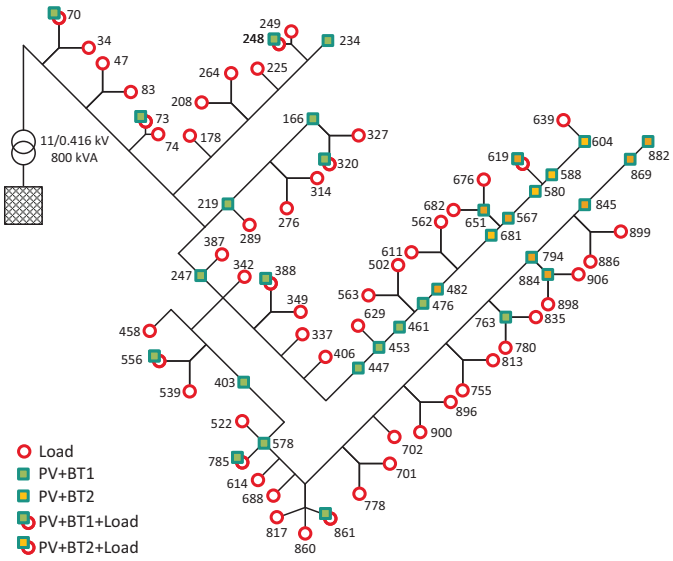

Fig. 6. Single-line diagram of the modified IEEE LV test feeder.

maximum ($SoC_{\max}$) SoC of the BESs are 10 % and 90 %, respectively; the charging/discharging efficiency is 0.95.

B. Long-Term Evaluation

The long-term impact of the ASs on the BES capacity degradation is investigated for a time period of $T^{\max}_{\text{LtP}} = 20$ years by adopting the methodology described in Section II. In this study, quasi-static simulations are conducted on the basis of multiple 24-h time simulations (Fig. 1) and the BES capacity degradation is evaluated considering $T_{\text{BES}} = 1$ year (Fig. 2). In particular, a six-day simulation pattern ($T_{\text{qss}} = 6$ days) is reiterated up to 365 days for every year T_{LtP} of the analysis: 24-h sunny and cloudy PV generation profiles with 1-min resolution are used. During a sunny day, the units of BT2 are employed to tackle voltage violations, and the units of BT1 remain idle. On the other hand, on a cloudy day BT1 units are used for PS and BT2 units provide both PS and VR services. The annual cloudy to sunny days ratio is considered 33.3 %, i.e., two cloudy days within the six-day simulation pattern. In the conducted analysis 55 load and 2 generation profiles are used derived from [17] and [9], respectively.

Considering the day-ahead planning algorithm, $sf = 20$ % and the available load profiles are randomly assigned at network load nodes to emulate the stochastic behaviour of LV consumers. The peak load demand of each node is maintained equal to the original one [17]. Regarding generation profiles, a uniform noise within the range of ± 5 % is added to the actual

TABLE I
PV INSTALLED CAPACITY

Node	kWp
70, 166, 234, 247, 248, 388, 403, 447, 453, 482, 556, 567, 580, 588, 619, 651, 763, 785, 845, 861, 869, 884	7.5
73, 219, 320, 461, 476, 578, 604, 681, 794, 882	15

TABLE II
BESS INSTALLED CAPACITY

BT1		
Node	kWh	kW
73, 219, 320, 461, 476, 578	3	4.5
70, 247, 166, 234, 248, 388, 403, 447, 453, 556, 785, 763, 861	1.5	2.25

BT2					
Node	kWh	kW	Node	kWh	kW
482, 681, 845	10	5	882	25	12.5
567, 580, 588	22.5	7.5	604	45	15
619, 651	30	7.5	794	5	5
869	15	7.5	884	5	2.5

adopted profiles. The capacity degradation of each BES for T_{BES} is determined considering an indicative $\overline{T}$ value equal to 20 °C. Regarding the properties of the examined PS and VR control strategies, it is assumed that the preferred SoC value at the end of the PS method is 50 %, $RR_{min} = -1.5$ W/s, $RR_{max} = 1.5$ W/s, $V_{\min}$ and $V_{\max}$ are 0.9 pu and 1.1 pu, respectively, and $V_1 = V_2 = 0.91$ pu, $V_3 = 0.92$ pu, $V_4 = 1.08$ pu, $V_5 = V_6 = 1.09$ pu.

Indicative daily SoC profiles of BT1 unit situated at node 73 (BT1-73) during a cloudy day of the 1st and the 12th year of the analysis are presented in Fig. 7a. It can be observed that the initial SoC (SoC_{init}) of both curves is 50 %. During the day, BT1-73 provides PS services and the SoC varies from 30 % to 60 %. Due to the SoC recovery signal, the SoC value at the end of the PS method is equal to SoC_{init} and the $\overline{SoC}$ operating value is 50 %. The impact of BT1-73 operation on the PV output power is depicted in Fig. 7b. It can be generally seen that similar PS is achieved, since the two smoothed profiles overlap. Small differences between the corresponding curves in Figs. 7a and 7b are because of the battery degradation through the years. Similar remarks are also derived for the rest BT1 units.

In Fig. 8, the SoC profiles of two indicative BT2 units are plotted for a six-day period of the 1st year. In particular, the SoC fluctuations observed in Fig. 8 during 56 - 66 h and 80 - 90 h are due to the provision of PS services during a cloudy day. The BES system of node 619 (BT2-619) presents a smoother SoC profile than the BT2 situated at node 794 (BT2-794). This is attributed to the fact that less active power is required by BT2-619 for PS compared to that for VR as this node is one of the most sensitive network nodes in terms of voltage variations. It can be also realized that the SoC profile is influenced by the forecasting load and generation error of the day-ahead planning algorithm used for the discharging process. More explicitly, as the load and generation forecasts

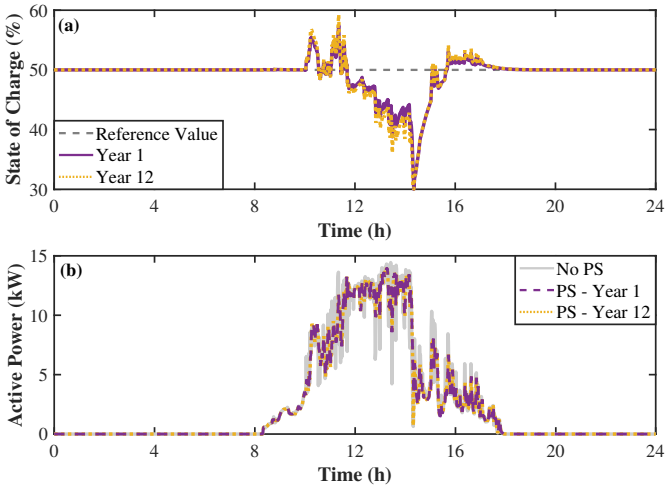

Fig. 7. (a) Daily SoC profile of BT1-73 (b) Daily PV output power profile during a cloudy day.

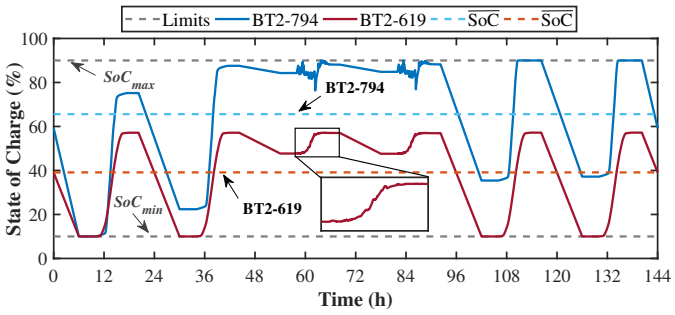

Fig. 8. Six-day SoC profile of indicative BT2 units.

for node 619 are on the safe side, BT2-619 sufficiently discharges and can absorb the required energy for the next day VR process, leading to a $\overline{SoC} = 39.12$ % over the six-day analysis period and consequently annually. This is not the case for BT2-794. The inaccurate prediction of the load and generation, results into an increased SoC, e.g., after 36 h, and consequently to $\overline{SoC} = 65.59$ %. In addition, the increase in $\overline{SoC}$ is also affected by the BES size. In particular, the size of BT2-794 is smaller than BT2-619, leading to a wider SoC operating range and in turn to a higher $\overline{SoC}$ as verified by Fig. 8. Comparing Figs. 7a and 8, it can be seen that BT1 units present lower SoC variations than BT2. This is attributed to the distinct decreased amounts of storage capacity required for PS compared to VR.

In Fig. 9, the capacity degradation of indicative BT1 and BT2 BESs is analysed. With respect to the results of Fig. 8, it can be observed that higher $\overline{SoC}$ operating values lead to accelerated BES aging. Specifically, it is shown that BT2-794 reaches the EoL at the 9th year. On the other hand a longer lifetime for BT2-619 is observed (four more years), due to the lower $\overline{SoC}$. As BT2-794 and BT2-619 present the highest and the lowest $\overline{SoC}$ of all BES units, i.e., 65.59 % and 39.12 %, respectively, it can be deduced that the available capacity of all BES units is reduced by 20 % after 9 - 13 years. In general, comparing the degradation rate of BT1 and BT2 units, it can be seen that the provision of both PS and VR services does

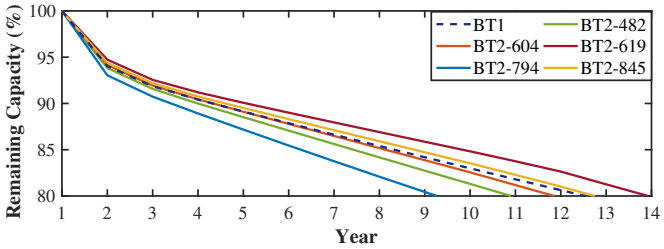

Fig. 9. BES capacity degradation.

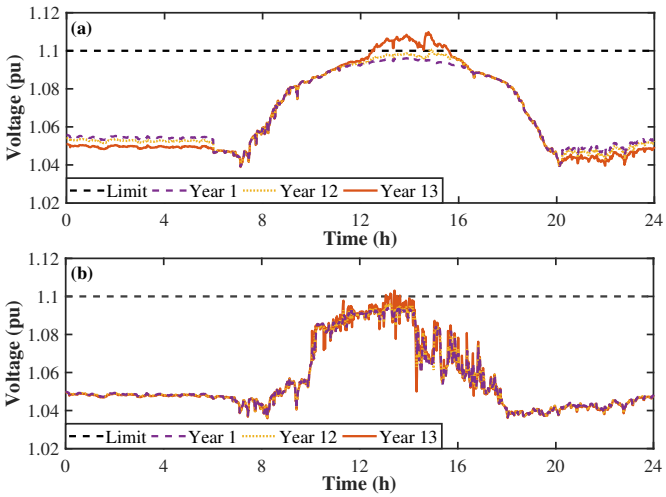

Fig. 10. Voltage profile of node 619 during (a) a sunny and (b) a cloudy day.

not explicitly result into decreased BES lifetime expectancy, e.g., BT2-619, BT2-845, compared to BT1 units.

Finally, in Figs. 10a and 10b, the daily profiles of the positive-sequence voltage at node 619 for different years are plotted for sunny and cloudy days, respectively. Differences in the voltage profiles of Fig. 10a during 20:25 h - 07:00 h, are due to the discharging process of BT2. In general, overvoltages are effectively mitigated during the 1^{st} year. Nevertheless, voltage violations are observed at the 12^{th} and 13^{th} year. This is attributed to the fact that most BT2 storage units (11 out of 13) have reached their EoL. Comparing a sunny to a cloudy day, it can be seen that overvoltages are more likely to be tackled in the latter case. Finally, the weakness of BT1 and BT2 to provide PS services during a cloudy day of the 13^{th} year is reflected to the corresponding voltage profiles characterized by intense fluctuations.

IV. Conclusion

A framework to evaluate the effectiveness of the provision of ASs by PV-BES systems is introduced in this paper. PV-BES units providing either VR and PS services or only PS services are considered. A BES aging algorithm is incorporated in the simulation model to improve the accuracy of the evaluation results. The long-term impact of the ASs on the BES capacity degradation is investigated on annual basis by conducting multiple 24-h quasi-static simulations.

From the analysis, it can be concluded that the provision of both PS and VR services does not necessarily lead to accelerated BES capacity degradation compared to the case where only PS is considered. In fact, BES aging is mainly influenced by the $\overline{SoC}$ operating value as higher $\overline{SoC}$ leads to accelerated BES capacity degradation. Respectively, $\overline{SoC}$ is affected by the forecast errors of the day-ahead planning algorithm for VR and the BES sizing characteristics; decreased BES size results into increased SoC range. However, increased BES sizing may lead to unnecessary investment costs; thus, optimum BES sizing must be determined on the basis of both the needs for AS provision and the effect of BES capacity degradation. Finally, to ensure efficient VR services for the whole lifetime of the PV units (20 years), at least one BES replacement must be considered.

References

[1] D. Olivares, A. Mehrizi-Sani, A. Etemadi, *et al.*, "Trends in Microgrid Control," *IEEE Trans. Smart Grid*, vol. 5, no. 4, pp. 1905–1919, 2014.

[2] A. Saint-Pierre and P. Mancarella, "Active Distribution System Management: A Dual-Horizon Scheduling Framework for DSO/TSO Interface Under Uncertainty," *IEEE Trans. Smart Grid*, vol. 8, no. 5, pp. 2186–2197, 2017.

[3] G. Kryonidis, E. Kontis, T. Papadopoulos, *et al.*, "Ancillary services in active distribution networks: A review of technological trends from operational and online analysis perspective," *Renew. Sustain. Energy Rev.*, vol. 147, p. 111198, 2021.

[4] M. Kabir, Y. Mishra, G. Ledwich, *et al.*, "Improving voltage profile of residential distribution systems using rooftop PVs and Battery Energy Storage systems," *Applied Energy*, vol. 134, pp. 290–300, 2014.

[5] H. Xu, A. Domínguez-García, V. Veeravalli, and P. Sauer, "Data-Driven Voltage Regulation in Radial Power Distribution Systems," *IEEE Trans. Power Syst.*, vol. 35, no. 3, pp. 2133–2143, 2020.

[6] Y. Huang, "Day-Ahead Optimal Control of PEV Battery Storage Devices Taking Into Account the Voltage Regulation of the Residential Power Grid," *IEEE Trans. Power Syst.*, vol. 34, no. 6, pp. 4154–4167, 2019.

[7] X. Li, D. Hui, and X. Lai, "Battery Energy Storage Station (BESS)-Based Smoothing Control of Photovoltaic (PV) and Wind Power Generation Fluctuations," *IEEE Trans. Sustain. Energy*, vol. 4, no. 2, pp. 464–473, 2013.

[8] L. Meng, T. Dragicevic, and J. Guerrero, "Adaptive Control Design for Autonomous Operation of Multiple Energy Storage Systems in Power Smoothing Applications," *IEEE Trans. Ind. Electron.*, vol. 65, no. 8, pp. 6612–6624, 2018.

[9] G. Kryonidis, A. Nousdilis, K. Pippi, and T. Papadopoulos, "Impact of Power Smoothing Techniques on the Long-Term Performance of Battery Energy Storage Systems," in *2021 56th Int. Univ. Power Eng. Conf. (UPEC)*, 2021, pp. 1–6.

[10] L. Maeyaert, L. Vandevelde, and T. Doring, "Battery Storage for Ancillary Services in Smart Distribution Grids," *J. Energy Storage*, vol. 30, p. 101524, 2020.

[11] B. Xu, A. Oudalov, A. Ulbig, *et al.*, "Modeling of Lithium-Ion Battery Degradation for Cell Life Assessment," *IEEE Trans. Smart Grid*, vol. 9, no. 2, pp. 1131–1140, 2018.

[12] T. Mai, A. Haque, P. Vergara, *et al.*, "Adaptive coordination of sequential droop control for PV inverters to mitigate voltage rise in PV-Rich LV distribution networks," *Electr. Power Syst. Res.*, vol. 192, p. 106931, 2021.

[13] L. Zhang, Z. Mu, and C. Sun, "Remaining Useful Life Prediction for Lithium-Ion Batteries Based on Exponential Model and Particle Filter," *IEEE Access*, vol. 6, pp. 17 729–17 740, 2018.

[14] "IEEE Standard for interconnection and interoperability of distributed energy resources with associated electric power systems interfaces," *IEEE Std 1547-2018 (Revision of IEEE Std 1547-2003)*, pp. 1–138, 2018.

[15] A. Nieslony, "Rainflow counting algorithm." [Online]. Available: https://de.mathworks.com/matlabcentral/fileexchange/3026-rainflow-counting-algorithm, Retrieved June 8, 2022.

[16] R. C. Dugan and D. Montenegro, *Reference guide: The Open Distribution System Simulator*, Technical Report 9.0.0., Electrical Power Research Institute, Washington, DC, 2020.

[17] "European Low Voltage Test Feeder," Apr. 01, 2021. [Online]. [Online]. Available: https://site.ieee.org/pes-testfeeders/resources/